Deep Autoregressive Models as Causal Inference Engines

Anonymous authors
Paper under double-blind review

Abstract

Existing causal inference (CI) models are often restricted to handling low-dimensional confounders and singleton actions. We propose an autoregressive (AR) CI framework capable of handling complex confounders and sequential actions commonly found in modern applications. Our approach accomplishes this using *sequencification*, which transforms data from an underlying causal diagram into a sequence of tokens. Sequencification not only accommodates training with data generated from a large class of DAGs, but also extends existing CI capabilities to estimate multiple causal quantities using a *single* model. We can directly compute probabilities from interventional distributions, simplifying inference and enhancing outcome prediction accuracy. We demonstrate that an AR model adapted for CI is efficient and effective in various complex applications such as navigating mazes, playing chess endgames, and evaluating the impact of certain keywords on paper acceptance rates.

1 Introduction

Modeling causal relationships is important across various fields for informed decision-making (Holland, 1986; Cochran & Rubin, 1973; Pearl, 2010). However, existing causal inference (CI) algorithms are often limited by their inability to handle high-dimensional covariates, actions, and outcomes (Louizos et al., 2017; Kumor et al., 2021; Im et al., 2021; Lu et al., 2022; Zhong et al., 2022). This work aims to address these shortcomings by designing a CI engine applicable for modern, complex data involving high-dimensional variables.

We propose to leverage autoregressive (AR) models for estimating causal effects. As demonstrated by large language models (LLMs), AR models can capture complex relationships and scale effectively to large datasets. Recent studies (Gupta et al., 2023; Zhang et al., 2024; Xu et al., 2024) show that fine-tuning pre-trained LLMs utilizes knowledge from an internet-scale text corpus, enhancing performance on various tasks.

We demonstrate that AR models serve as an effective and efficient statistical engine by treating observations as part of a data-generating process. To achieve this, we propose a method called *sequencification* for representing data based on a known underlying causal diagram. A *single* model trained on sequencified data can utilize learned statistical estimates to answer a variety of causal questions. During inference, we can efficiently sample high-dimensional confounders and actions, enabling Monte Carlo estimation to approximate causal effects.

We conduct empirical studies on causal effect estimation across a variety of exemplar tasks, such as navigating mazes, playing chess endgames, and evaluating the impact of specific keywords on paper acceptance rates. Our experiments show that AR models can (1) infer causal effects involving high-dimensional variables, (2) generalize to unseen confounders and action sequences, and (3) leverage pre-trained LLMs to accurately answer text-based causal questions. The results support the potential of AR models to solve a broader array of CI problems.

2 Related work

Previous work has explored the use of AR models for estimating causal effects. Here, we provide a brief overview of the relevant studies.

Sequencification for statistical engines. Various machine learning fields have used linearized representations for tasks. In natural language processing (NLP), linearization (which we refer to as sequencification) is used to convert a syntactic tree into a sequence for building language model-based parsers (Vinyals et al., 2015; Liu et al., 2022; Sheng et al., 2023). In reinforcement learning (RL), an episode can be encoded as a sequence of states, actions, and rewards. An autoregressive model is then trained on these sequences to capture relationships among the variables (Chen et al., 2021; Janner et al., 2021). These instances suggest that AR models trained on sequencified data can effectively learn statistical dependencies among multiple high-dimensional variables.

Language models as causal engines. A key challenge in CI in high-dimensional spaces is satisfying positivity constraints (D'Amour et al., 2021; Tu & Li, 2022; Egami et al., 2022; Gui & Veitch, 2022). Despite this limitation, previous studies have used techniques from NLP, such as topic models (Sridhar & Getoor, 2019; Mozer et al., 2020), latent variable models (Keith et al., 2020), and contextual embeddings (Veitch et al., 2019; 2020), to produce low-dimensional embeddings that can satisfy positivity.

In addition to using NLP techniques to reduce the dimensionality of observations, natural language can also serve as a proxy for observed confounders. For example, Roberts et al. (2020) apply a text-matching algorithm using contextual embeddings and topic models to estimate causal effects based on proxy texts. With sufficiently large models and text corpora, LLMs can also generalize to previously unseen knowledge (Chowdhery et al., 2023). Thus, we leverage pre-trained LLMs to capitalize on prior model knowledge and enhance the performance of statistical inference engines.

Deep learning for causal engines. Various deep neural network architectures have been proposed for CI. Representation learning for CI often incorporates a regularization term that enhances generalization for counterfactual actions (Shalit et al., 2017; Johansson et al., 2018; Wang & Jordan, 2021). Deep latent variable CI models learn stochastic latent variables to model potential outcomes with a richer distribution (Louizos et al., 2017; Kocaoglu et al., 2017; Im et al., 2021).

For deep autoregressive models, Monti et al. (2020) introduce an AR flow model that learns an invertible density transformation between variables. Their approach enables direct computation of interventional and counterfactual distributions without the need for complex latent variable manipulations. Garrido et al. (2021) use neural AR density estimators (Larochelle & Murray, 2011) to model causal mechanisms and predict causal effects using Pearl's do-calculus (Pearl, 2009).

Causal Generative Models. Another approach to CI models data as part of a generative process and learns a causal generative model. These methods typically parameterize relationships in a known causal diagram using neural networks. For causal effect identification and estimation, Xia et al. (2023) use neural causal models trained via gradient-based optimization with a minimization-maximization objective. Rahman & Kocaoglu (2024) introduce a modular learning framework for optimizing causal generative models in semi-Markovian settings by decomposing the data distribution into c-factors (Tian & Pearl, 2002). Their method can use pre-trained generative models to learn individual conditional distribution components.

Existing limitations. Previous works exhibit notable weaknesses compared to our approach. First, most methods are validated only on low-dimensional variables (tens of dimensions) and singleton actions. In contrast, our AR model is designed to handle high-dimensional confounders and sequential actions where the number of possible sequences grows exponentially. This makes it applicable to causal diagrams with a large number of variables. Second, prior studies often focus on estimating specific causal effects or learning generative models by optimizing individual components of the causal structure. We instead use a *unified* end-to-end AR model that can estimate multiple identifiable causal queries. Third, we extend existing CI capabilities by leveraging pre-trained language models for setting where autoregressive domain knowledge is essential for accurate inference (e.g. NLP).

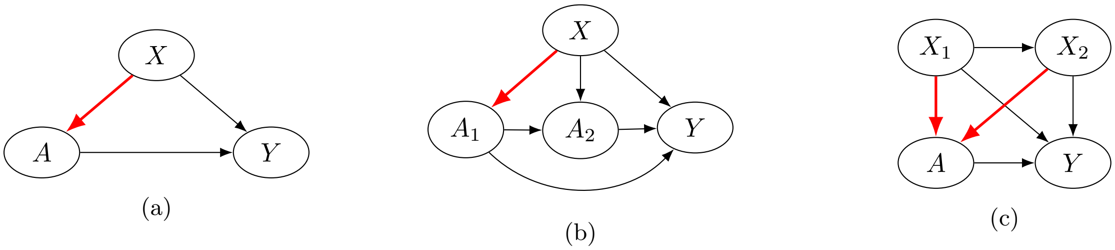

(a)

(b)

(c)

Figure 1: Causal diagrams illustrating interventions on the action (a), partial action (b), and when conditioning on a prefix of the confounders (c), where X, A, and Y denote the confounders, actions, and outcome respectively. Bolded red arrows indicate the pathways blocked by the corresponding intervention. Potential outcomes can be computed using the backdoor adjustment formula for each scenario.

3 Background

This section outlines the background knowledge of causal effect estimation and language models necessary for understanding our methodology.

3.1 CI problem formulation

We study interactions between the following set of variables: an observable confounder X, action A, and outcome Y. Causal relationships are represented as a directed acyclic graph (DAG), where edges denote direct effects (cf. Figure 1a). By applying the backdoor adjustment formula (Pearl, 2009), we can compute the potential outcome resulting from an intervention on the action:

$$\mathbb{E}_Y[Y \mid \mathsf{do}(A=a)] \coloneqq \sum_{x,y} y \cdot p(Y=y \mid A=a, X=x)p(X=x). \tag{1}$$

The notation $\mathsf{do}(A=a)$ represents an intervention on A, setting its value to a. Typically, the confounder X is assumed to be low-dimensional to avoid computing density estimates $p(x)$ in high dimensions. Our goal is to model causal effects when typical assumptions in prior CI work are violated, including settings with complex confounders and combinatorially large action spaces.[1]

3.2 Language models

Language models (LMs) are designed to predict and generate text by learning linguistic patterns from a training corpus. Let $\mathbb{W}$ denote the vocabulary of the text corpus, which includes special $\langle\texttt{start}\rangle$ and $\langle\texttt{end}\rangle$ tokens. LMs estimate the probability of a sequence of tokens $\mathbf{w} = (w_1, \cdots, w_T) \in \mathbb{W}^T$ in an autoregressive manner. Let $\mathbf{w}_{1:t}$ represent the first t tokens in $\mathbf{v}$. The probability of the sequence $\mathbf{w}$ is decomposed into the product of next-token probabilities:

$$p(\mathbf{w}) = p(\langle\texttt{start}\rangle) \cdot \prod_{t=1}^{T} p(w_t|\mathbf{w}_{1:t-1}) \cdot p(\langle\texttt{end}\rangle|\mathbf{w}).$$

4 Language models as statistical inference engines

As suggested by Equation 1, CI requires accurate estimation of statistical quantities to calculate causal effects. In this section, we describe how an AR model can be adapted into a statistical inference engine for any DAG involving a set of confounders, actions, and outcomes using sequencification.

---

[1] A combinatorially large action space refers to the number of possible action sequences.

4.1 Causal graphs

We assume the underlying causal DAG $\mathcal{G} = (\mathcal{V}, \mathcal{E})$ is known, where the vertices $V_i \in \mathcal{V}$ represent random variables and the edges $E_{i \to j} \in \mathcal{E}$ denote conditional dependencies. The joint probability distribution is

$$p_{\mathcal{G}}(V_1, V_2, \ldots, V_M) = \prod_{i=1}^{M} p_{\mathcal{G}}(V_i \mid \mathrm{Pa}(V_i)),$$

where $\mathrm{Pa}(V_i) = \{V_j \in \mathcal{V} \mid E_{j \to i} \in \mathcal{E}\}$ is the set of parent nodes of V_i. We assume that the graph $\mathcal{G}$ is fully specified and that all variables within $\mathcal{G}$ are observed.

4.2 Sequencification

Suppose V_i takes the value $\mathbf{v}_i$ from its corresponding distribution. Let string$(\cdot)$ be an injective function that maps $\mathbf{v}_i$ to a sequence of tokens: $\mathrm{string}(\mathbf{v}_i) = (\langle \texttt{start}_i \rangle, w_1, w_2, \ldots, w_{L_{\mathbf{v}_i}})$. Here, $\langle \texttt{start}_i \rangle$ is a special token indicating the beginning of the string representation for $\mathbf{v}_i$, and $L_{\mathbf{v}_i}$ is the length of $\mathrm{string}(\mathbf{v}_i)$ excluding the $\langle \texttt{start}_i \rangle$ token. We define $\langle \texttt{start}_i \rangle$ uniquely for each i so that each random variable can be uniquely identified from its string representation by its corresponding initial token.

Let $\mathbf{t} = (V_{i_1}, V_{i_2}, \ldots, V_{i_M})$ be a permutation of the random variables. We say $\mathbf{t}$ is a *topological ordering* if V_i precedes V_j in the ordering for all edges $E_{i \to j}$. Let $\mathcal{T}$ denote the set of all topological orderings.[2] Consider N samples drawn from the underlying causal diagram $\mathcal{G}$: $(\mathbf{v}_1^{(n)}, \mathbf{v}_2^{(n)}, \cdots, \mathbf{v}_M^{(n)}) \sim p_{\mathcal{G}}(V_1, V_2, \cdots, V_M)$ for $n = 1, \ldots, N$. For each sample, we construct a string $\mathbf{s}^{(n)}$ by concatenating the string representations of all random variables according to a topological ordering $\mathbf{t}^{(n)}$ selected uniformly at random from $\mathcal{T}$. Formally, $\mathbf{t}^{(1)}, \mathbf{t}^{(2)}, \ldots, \mathbf{t}^{(N)} \overset{i.i.d.}{\sim} \mathrm{Uniform}(\mathcal{T})$ and

$$\mathbf{s}^{(n)} = \ \mathrm{string}(\mathbf{v}_{i_1}^{(n)}) \oplus \mathrm{string}(\mathbf{v}_{i_2}^{(n)}) \oplus \cdots \oplus \mathrm{string}(\mathbf{v}_{i_M}^{(n)}) \oplus \langle \texttt{end} \rangle,$$

where $\mathbf{t}^{(n)} = (V_{i_1}, V_{i_2}, \ldots, V_{i_M})$ and $\oplus$ denotes string concatenation. We refer to the process of converting observed samples into a sequence of tokens as *sequencification.*

Sequencification supports any data that can be transformed into a linear sequence of tokens. For example, tokens may represent specific values for numerical (e.g., binary) data or subwords for text, depending on the problem domain. Our approach can also handle mixed data modalities, as different variables may have separate tokenization strategies.

4.3 Randomized topological orderings

We randomize over topological orderings consistent with the causal graph to obtain robust estimates of conditional probabilities. For instance, if a node in the graph has multiple independent parents, randomizing the order in which the parents are sequenced helps prevent the model from overfitting to any particular ordering. As a result, different samples may be concatenated using distinct topological orderings. However, because the data is generated by ancestor sampling $\mathbf{v}_i^{(n)} \mid \mathrm{Pa}(\mathbf{v}_i^{(n)})$, values that causally influence $\mathrm{string}(\mathbf{v}_i^{(n)})$ will always appear earlier in $\mathbf{s}^{(n)}$.

A natural question that may arise is how to obtain a good estimate when samples are sequencified according to different topological orderings. This is achieved by using the special $\langle \texttt{start}_i \rangle$ token at the start of each variable V_i during sequencification, which indicates its position in the sequence (regardless of the topological ordering used).

---

[2] $\mathcal{T}$ is guaranteed to be non-empty because all DAGs have a topological ordering.

4.4 Autoregressive statistical inference engines

After sequentification, we can train an AR language model, parameterized by θ, on the sequencified dataset $D = \{\mathbf{s}^{(1)}, \mathbf{s}^{(2)}, \ldots, \mathbf{s}^{(N)}\}$ by the minimizing negative log-likelihood:

$$\mathcal{L}(\theta) = -\frac{1}{N}\sum_{n=1}^{N} \log p_\theta(\mathbf{s}^{(n)}) = -\frac{1}{N}\sum_{n=1}^{N}\sum_{t=1}^{|\mathbf{s}^{(n)}|} \log p_\theta\left(\mathbf{s}_t^{(n)} \;\middle|\; \mathbf{s}_{1:t-1}^{(n)}\right) \tag{2}$$

where $|\cdot|$ denotes the length of a string and $\mathbf{s}_t^{(n)}$ is the t^{th} token in $\mathbf{s}^{(n)}$. The trained model can estimate any conditional probability on $\mathcal{G}$ by computing $p_{\mathcal{G}}(V_i \mid \mathrm{Pa}(V_i)) \simeq p_\theta(\mathbf{v}_i \mid \mathrm{Pa}(\mathbf{v}_i))$. This is efficiently done by autoregressively traversing the sequence and calculating next-token probabilities using Monte Carlo estimation over the topological orderings.

5 Language models as causal inference engines

In this section, we illustrate how to infer causal effects by leveraging statistical quantities from a trained AR model, thereby transforming it into a causal inference engine. After learning the conditional distribution over $\mathcal{G}$ using an AR model, we can estimate causal quantities by deriving the appropriate identification formula from the known causal diagram. Sequencification, combined with knowledge of $\mathcal{G}$, allows us to estimate various causal effects.

5.1 Estimating causal quantities

We express the CI problem as a language modeling task. Given our DAG that consists of three variables (the observed confounder X, action A, and outcome Y), we sequencify the data as follows:

$$\mathbf{s}^{(n)} = \mathrm{string}(\mathbf{x}^{(n)}) \oplus \mathrm{string}(\mathbf{a}^{(n)}) \oplus \mathrm{string}(y^{(n)}) \oplus \langle \texttt{end} \rangle.$$

In our formulation, $\mathbf{x}^{(n)}$ and $\mathbf{a}^{(n)}$ can be high-dimensional vector values and the action space can be combinatorially large. Without loss of generality, we treat the outcome variable Y as a scalar, represented as a single token.

We can use the trained AR model to compute the distribution of Y after intervening on A. This is typically intractable when X is high-dimensional because computing a non-parametric density estimate is exponential in the number of dimensions. However, we can efficiently approximate the interventional distribution by sampling from $p_\theta(X)$ and applying Monte Carlo estimation.

$$p_\theta(Y = y \mid \mathsf{do}(A = \mathbf{a})) = \sum_{\mathbf{x}} p_\theta(y \mid A = \mathbf{a}, \mathbf{x}) p_\theta(\mathbf{x}) \simeq \frac{1}{S}\sum_{s=1}^{S} p_\theta(y \mid A = \mathbf{a}, \boldsymbol{x}^{(s)}), \tag{3}$$

where $\boldsymbol{x}^{(s)} \sim p(X)$.

Furthermore, we can intervene on a prefix subsequence of A even when the action space is large. By expressing $A = A_1 \oplus A_2$ and marginalizing out A_2, we can compute the effect of intervening on only A_1.

$$p(Y = y \mid \mathsf{do}(A_1 = \mathbf{a}_1)) = \sum_{\mathbf{x}}\sum_{\mathbf{a}_2} p_\theta(y \mid A_1 = \mathbf{a}_1, A_2 = \mathbf{a}_2, \mathbf{x}) p_\theta(\mathbf{a}_2 \mid \mathbf{a}_1, \mathbf{x})\, p_\theta(\mathbf{x}) \tag{4}$$

$$\simeq \frac{1}{S}\sum_{s=1}^{S} p_\theta(y \mid \mathbf{a}_1, \boldsymbol{a}_2^{(s)}, \boldsymbol{x}^{(s)}), \tag{5}$$

where $\boldsymbol{x}^{(s)} \sim p(X)$ and $\boldsymbol{a}_2^{(s)} \sim p(A_2 \mid \mathbf{a}_1, \boldsymbol{x}^{(s)})$. For combinatorially large action spaces, Equation 4 is generally intractable because the marginalization requires exponentially many operations.

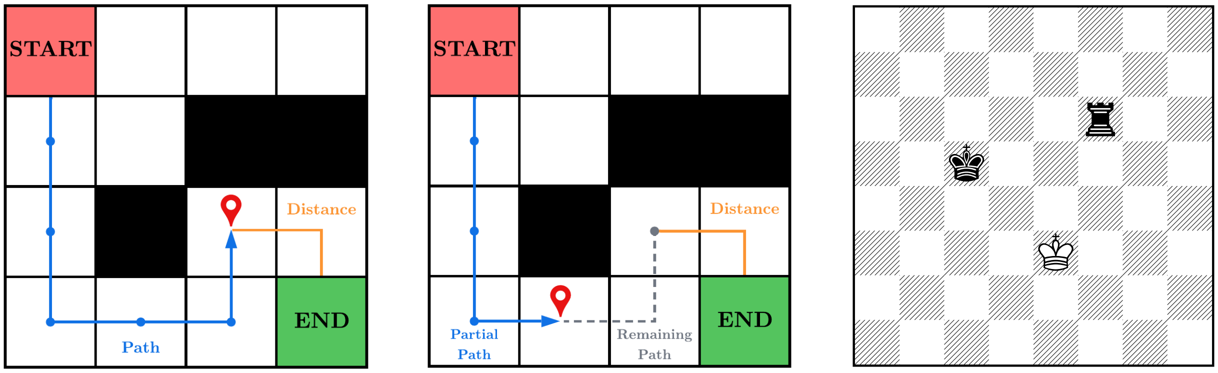

(a) (b) (c)

Figure 2: Illustrations of the maze and chess experimental settings. In the maze experiment, we address two questions: what is the potential outcome given (a) a complete path, and (b) a partial path? The blue path represents the intervention, gray indicates a potential remaining path after a partial intervention, and orange denotes the distance to the end. The chess experiment aims to determine which pieces Black should move to checkmate White the quickest. In the example position shown in (c), the probability of moving the Black king is 0.5, 0.25, and 0.8 with the RCT, non-RCT$_1$, and non-RCT$_2$ policies respectively.

Similarly, we can condition on a prefix of the confounder by letting $X = X_1 \oplus X_2$ and marginalizing out X_2.

$$p(Y = y \mid \mathsf{do}(A = \mathbf{a}), \mathbf{x}_1) = \sum_{\mathbf{x}_2}^{X_2} p_\theta(y \mid A = \mathbf{a}, \mathbf{x}_2, \mathbf{x}_1)\, p_\theta(\mathbf{x}_2 \mid \mathbf{x}_1) \tag{6}$$

$$\simeq \frac{1}{S} \sum_{s=1}^{S} p_\theta(y \mid A = \mathbf{a}, \boldsymbol{x}_2^{(s)}, \mathbf{x}_1) \tag{7}$$

where $\boldsymbol{x}_2^{(s)} \sim p(X_2 \mid X_1 = \mathbf{x}_1)$. The causal diagrams for these scenarios are shown in Figure 1. Note that we can only intervene on prefixes of the action A_1 (or condition on prefixes of the confounder X_1) because this ensures the marginalization step samples A_2 (or respectively X_2) conditioned on preceding variables.

We emphasize that all causal quantities can be computed by a *single* language model trained on sequencified observations. Our approach enables efficient sampling and computation of conditional $p(Y \mid A = \mathbf{a})$, interventional $p(Y \mid \mathsf{do}(A = \mathbf{a}))$, partial interventional $p(Y \mid \mathsf{do}(A = \mathbf{a}_1))$, and conditional interventional $p(Y \mid \mathsf{do}(A = \mathbf{a}), X_1 = \mathbf{x}_1)$ distributions, all using a unified model. This provides an end-to-end framework for computing a variety of causal queries using a single model.

While the partial interventional distribution $p(Y \mid \mathsf{do}(A_1 = a_1))$ is computable by effectively discarding A_2, training an AR model on sequencified data that explicitly includes A_1 and A_2 is more flexible. Our approach can efficiently estimate not only partial interventional distributions but also interventions on A_1 and A_2 simultaneously, providing a unified framework for handling multiple causal queries. A similar argument holds for partially conditioning on the confounders.

6 Experiments

We demonstrate the effectiveness of our approach in estimating causal effects for sequential actions and high-dimensional confounders while also assessing robustness to distribution shifts. Our experiments showcase the ability to (1) infer potential outcomes with sequential actions and high-dimensional confounders, (2) efficiently approximate potential outcomes via Monte Carlo sampling, and (3) leverage knowledge from a pre-trained LLM. We evaluate our method across three environments: a maze setting for navigational decision-making, a chess environment analyzing strategic moves in king vs. king-rook endgames, and the `PeerRead` dataset which examines the impact of theorem presence on academic paper acceptance.

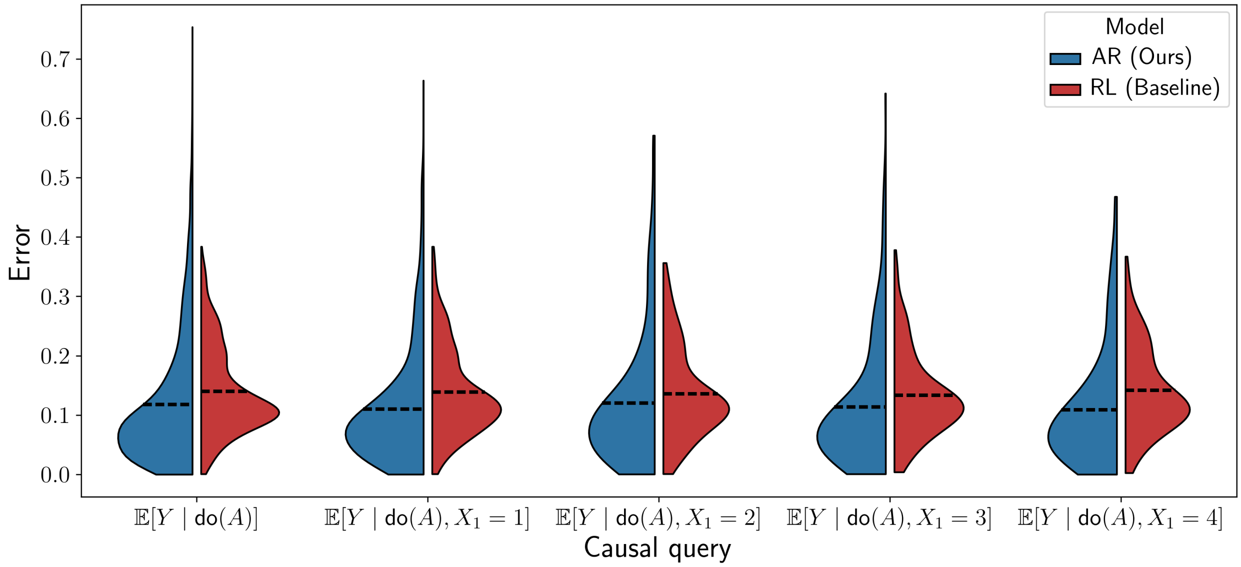

Figure 3: Error distribution of potential outcome estimates for our AR model (blue) and the offline RL baseline (green). We compute the effect of intervening on the complete path with and without conditioning on the starting row X_1. The plot depicts the distribution of errors across all 4096 possible paths of length six, while the black dashed line represents the mean error. The AR and RL models exhibit comparable performance across all settings, with our AR model performing marginally better.

The maze experiments demonstrate that our unified AR model can estimate interventions, partial interventions, and conditional interventions using Equations 3, 4, and 6, respectively. In contrast, a traditional offline reinforcement learning (RL) model fails to capture all three causal effects. In the chess experiments, we highlight the effectiveness of our method in estimating effects via Monte Carlo approximation using Equation 5 and its robustness to distribution shifts in the test data. Finally, the `PeerRead` setting demonstrates that the AR model can estimate effects in high-dimensional confounder scenarios and leverage pre-trained language models to improve text-based analysis.

These diverse settings enable a comprehensive evaluation of the effectiveness and robustness of our approach for CI. All AR models are trained using a vanilla transformer (Vaswani et al., 2017) unless otherwise specified. Additional details on the model architecture and training process can be found in Appendix A.[3]

6.1 Maze navigation experiments

In this experiment, we show that a unified AR model can estimate multiple types of causal queries using Equations 3, 4, and 6. Compared to a baseline offline RL model, our approach offers greater flexibility for causal inference tasks.

We generate a synthetic maze dataset to analyze the causal effect of traversing different paths. The goal is to determine the distance to the exit after following a given path. The confounding variable X represents the starting position, the action A is a sequence of moves, and the outcome Y denotes the distance from the final position to the exit.[4] We evaluate potential outcomes when intervening on a complete path (cf. Figure 2a) or partial path (cf. Figure 2b). The obstacle positions are fixed but are not known to the model. Our experiments demonstrate that a *single* AR model can accurately estimate interventional, partial interventional, and conditional interventional distributions.

The end position is fixed at the bottom-right corner, while the starting position is randomly selected from open spaces. The probability of choosing a starting square is proportional to its distance from the endpoint.

---

[3] All code and datasets will be made publicly available upon publication.

[4] Y is the shortest possible distance in the maze while avoiding obstacles, not necessarily the Hamming distance.

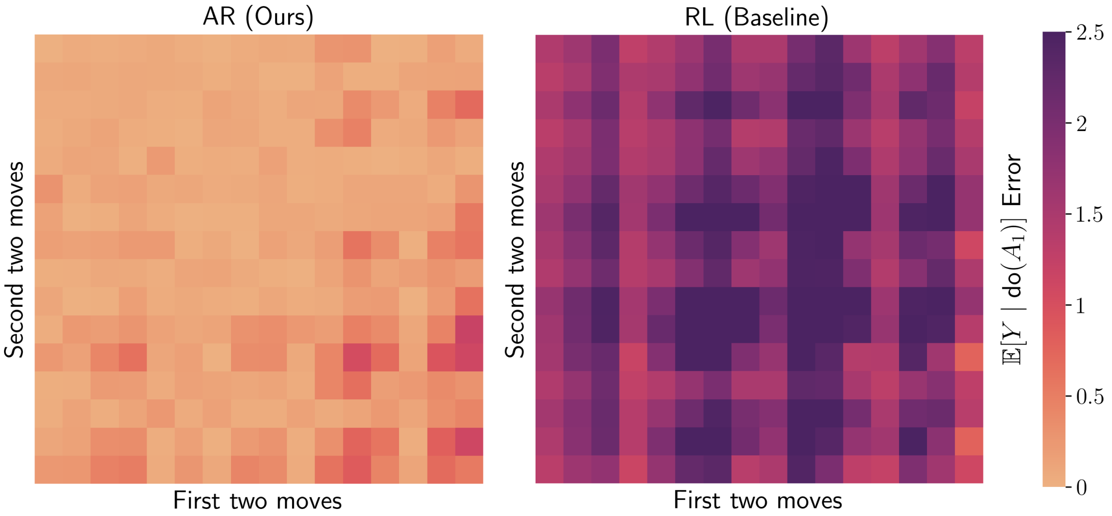

Figure 4: Heatmap illustrating the error distribution of potential outcome estimates when intervening on the first four moves in the path. Each row represents all possible actions for the first two moves, while each column represents all possible subsequent two moves. Our AR model accurately estimates potential outcomes for all four-move sequences by learning $p(\mathbf{a}_2 \mid \mathbf{a}_1, \mathbf{x})$ to compute the estimate. The offline RL baseline exhibits significant errors across nearly all interventions.

Moves in the path are determined by selecting a direction based on the current position. Let the current square be in the ith row from the top and the jth column from the left. The next move is chosen according to the probabilities:

$$p_{\text{up}} = p_{\text{left}} = 0.1, \quad p_{\text{right}} = \frac{0.8i}{i+j}, \quad p_{\text{down}} = \frac{0.8j}{i+j}.$$

This policy encourages paths to move towards the bottom-right corner. All actions are possible at any position, however moves that would collide with obstacles or walls in the maze are treated as no action. Paths are fixed to contain exactly six moves.

We train an AR model on sequencified data and use a deep Q-learning (DQL) model as an offline reinforcement learning (RL) baseline. The AR model is given only the starting position and must infer the effect of each move along the path. The DQL model follows the standard RL framework, where the current position is known after each move.

6.1.1 Causal inference using sequential actions

We estimate potential outcomes for all paths of length six in a 4×4 maze using Equation 3. Additionally, we compute potential outcomes conditioned on the starting row (from the top of the maze) $X_1 \in \{1, 2, 3, 4\}$ using Equation 6. Ground truth values are computed using the corresponding equations with the outcome outcome $\mathbb{E}_Y[Y \mid a, x]$ equal to the true number of additional moves required to reach the end of the maze after starting in position x and taking path a. For the RL method, we predict the potential outcome as the q-value after taking the final action in the intervention.

Figure 3 presents the error distribution for potential outcome estimates across all paths. In all settings, both models produce estimates that closely match the ground truth. Our AR model performs comparably to the offline RL baseline in terms of mean estimation error. The AR error distribution exhibits a large tail, which can be attributed to differences in training setups. Unlike the RL model, which receives the intermediate state after each move, the AR model must infer state transitions from scratch. Even without this knowledge, our model achieves slightly better overall performance, with a higher proportion of interventions yielding small errors. These results demonstrate that our approach can accurately predict both intervention and conditional intervention queries.

6.1.2 Causal inference using partial actions

In addition to computing complete interventions, we can also intervene on partial actions. To illustrate this scenario, we estimate potential outcomes when intervening on the initial moves in a path. Specifically, we decompose $A = A_1 \oplus A_2$, where A_1 represents the first four moves and A_2 the remaining two moves, and compute $p(Y \mid \mathsf{do}(A_1 = \mathbf{a}_1))$. Ground truth potential outcomes are calculated using Equation 4 by marginalizing over all possible remaining paths A_2. For the RL method, we intervene on the first four moves, while the remaining path is determined according to the learned policy.

Figure 4 shows the error distribution for potential outcome estimates across all possible four-move interventions. Our AR model accurately computes these estimates using Equation 4. In contrast, the offline RL model does not learn the distribution $p(\mathbf{a}_2 \mid \mathbf{a}_1, \mathbf{x})$ but instead optimizes for the best policy. As a result, it fails to predict partial interventions without modifications, such as discarding information about A_2 during training. This highlights the greater flexibility of our AR framework, which allows interventions on any subset of initial moves with a single model.

6.2 Chess endgame experiments

In this section, we evaluate the performance of our AR model with Monte Carlo sampling, following Equation 5, and assess its robustness to distribution shifts. To explore these aspects in a more complex two-player setting, we use a synthetic chess dataset featuring king vs. king-rook endgames, where White moves first and Black holds the rook. We demonstrate that our AR model can accurately compute causal effects and identify optimal action sequences by comparing potential outcome estimates. Additionally, we leverage Monte Carlo sampling to refine estimates when only partial data is available and introduce a distribution shift between training and testing data to assess generalization.

To formulate our causal query, we ask: on average, across all starting positions, which pieces should Black move on the first two turns to checkmate White as quickly as possible? Our question aims to uncover a general strategy for king vs. king-rook endgames, much like how controlling the center is a fundamental principle in the opening. More broadly, it parallels causal inference in scenarios with multiple initial conditions, where the objective is to identify the most effective strategy across a wide range of situations rather than an individual configuration.

Each endgame comprises a two-move chess game, potentially incomplete. The covariate X is the initial piece positions. The action $A = a_1, a_2, a_3, a_4$ represents alternating White and Black moves. Since we consider Black's perspective, we are interested in causal quantities involving a_2 and a_4. We assume Black plays optimally after selecting which piece to maneuver, so each action only dictates whether to move the king or the rook, but not to which location. The outcome variable y is the number of additional moves required to checkmate with optimal play.[5] Formally, we are interested in finding

$$(a_2^*, a_4^*) = \underset{a_2, a_4 \in \{\texttt{king}, \texttt{rook}\}}{\arg\min} \mathbb{E}_Y[Y \mid \mathsf{do}(a_2, a_4)] = \underset{a_2, a_4 \in \{\texttt{king}, \texttt{rook}\}}{\arg\min} \sum_{x,y} y \cdot p(Y = y \mid x, a_2, a_4) p(x).$$

We evaluate the ground truth outcome using the chess engine Stockfish[6]. An example endgame is shown in Figure 2c.

We construct three training datasets: one Randomized Control Trial (RCT), which selects each action uniformly at random between moving the king or the rook, and two non-RCT datasets, labeled non-RCT$_1$ and non-RCT$_2$, with distinct action policies. The policy functions for non-RCT$_1$ and non-RCT$_2$ are defined as follows, where d is the Hamming distance between the kings:

$$\pi_1(a_2, a_4 = \text{king}) = \frac{d}{16}, \quad \pi_2(a_2, a_4 = \text{king}) = \begin{cases} 0.8 & \text{if black king is in center } 4 \times 4 \text{ square} \\ 0.2 & \text{otherwise} \end{cases}$$

---

[5] In the event of a draw, the outcome is set to 50 due to the 50-move rule.

[6] Stockfish is available at `https://github.com/official-stockfish/Stockfish`.

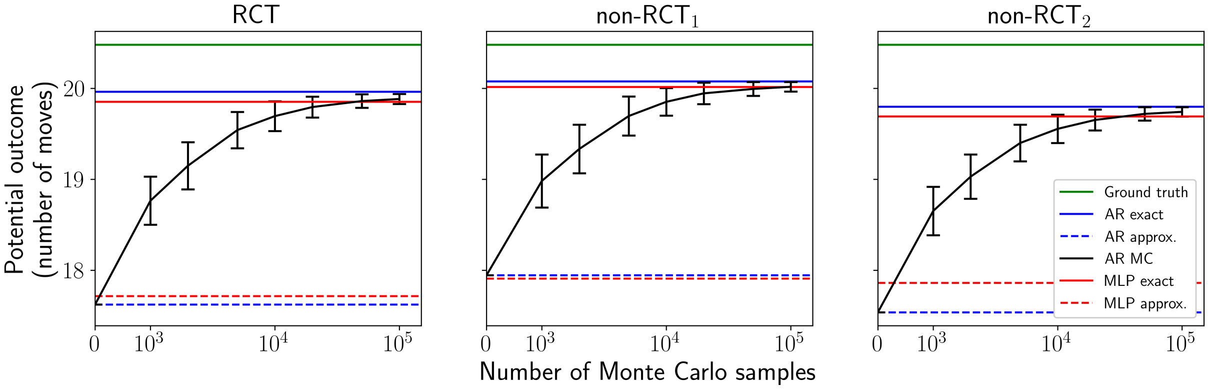

Figure 5: Potential outcome estimates for rook-king. The *exact model estimate* uses all 223,660 valid starting positions as test samples, while the *approximate* and *Monte Carlo estimates* use 1,000 randomly selected samples. Each Monte Carlo estimate was repeated 1,000 times, with error bars representing one standard deviation. By sampling from $p_\theta(X)$, the AR Monte Carlo estimate approaches the AR exact estimate. In contrast, the MLP model cannot perform sampling on $p_\theta(X)$.

π_1 encourages the two kings to be closer while π_2 pushes the Black king towards the edge of the board, both of which are required for checkmate. We use different RCT and non-RCT data to demonstrate robustness in the presence or absence of $X \to A$ and under varying action assignment mechanisms.

The testing dataset consists of all 223,660 valid starting positions. To assess out-of-distribution generalization, we use two distinct policies for White in the training and testing phases. White plays uniformly at random over non-optimal moves (unless no such legal moves are available) during training and plays optimally at test time. This introduces a distribution shift, which we use to evaluate generalization and robustness to new settings. Additionally, we show that our proposed AR framework produces more accurate causal estimates by using Monte Carlo sampling from $p_\theta(X)$ when given only a subset of the testing data.

We compute the ground truth potential outcomes for all actions and compare them with three different model estimates: the *exact model estimate* using the entire test dataset, the *approximate model estimate* using a subset of the test data, and the *Monte Carlo model estimate*, which also uses the same data subset but additionally generates samples from the model. The approximate and Monte Carlo estimates reflect real-world scenarios, where obtaining a large number of RCT samples is often difficult. We train a non-autoregressive multilayer perceptron (MLP) as a baseline for comparison.

Figure 5 presents our three model estimates for the AR and MLP model. As the number of samples in the Monte Carlo approximation increases, the potential outcome estimate converges to the exact estimate. Our results demonstrate that potential outcomes can be efficiently and accurately approximated with an AR model using only a fraction of the test data. Additionally, there is a gap between the AR exact model estimate and the ground truth, caused by the distribution shift in how White plays between the training and test data. The potential outcomes for the remaining actions are provided in Appendix B. By comparing all potential outcome estimates, we can answer our causal question and conclude that, aggregated across all starting positions, moving the rook twice initially is the best strategy for Black.

6.3 `PeerRead` experiments

We use the `PeerRead` dataset (Kang et al., 2018) to estimate causal effects in a semi-realistic setting with high-dimensional text confounders. Our results demonstrate that an AR model can leverage pre-trained language models to enhance CI in text-based settings. The dataset consists of paper draft submissions to top computer science conferences, such as NeurIPS, ICML, and ICLR, along with their acceptance or rejection decisions. We investigate the impact of including “theorems” on acceptance likelihood and evaluate how well our model captures this causal effect. Building on prior work, we focus on computational linguistics, machine learning, and artificial intelligence papers submitted between 2007 and 2017 (Veitch et al., 2020).

Table 1: `PeerRead` ATT performance across low, medium, and high confounding levels, with relative error indicated in parentheses. Our Deep Autoregressive Causal Inference Engine BERT (DARCIE-BERT) model achieves the lowest relative error, followed by DARCIE-GPT. Both models show significant improvement over other methods. Training DARCIE-GPT from scratch fails to identify causal effects due to its lack of understanding of the text.

	Confounding level		
	Low ($\beta = 1$)	Medium ($\beta = 5$)	High ($\beta = 25$)
Ground truth	0.062	0.059	0.028
Computed biased	**0.065 (4.8%)**	0.097 (68%)	0.160 (470%)
Reported biased (Veitch et al., 2020)	0.08 (30%)	0.15 (150%)	0.16 (471%)
MLP $\hat{\psi}^{Q}$	0.05 (20%)	0.10 (70%)	0.30 (970%)
C-BERT $\hat{\psi}^{\text{plugin}}$	0.10 (61%)	0.09 (53%)	0.05 (78%)
C-BERT $\hat{\psi}^{Q}$	0.09 (45%)	0.07 (19%)	0.04 (42%)
DARCIE-GPT (No pre-train)	0.001 (98%)	0.002 (97%)	0.001 (96%)
DARCIE-BERT (Ours)	0.052 (16%)	**0.050 (15%)**	**0.023 (18%)**
DARCIE-GPT (Ours)	0.050 (20%)	0.044 (25%)	0.020 (29%)

The covariate X represents the paper's abstract text, the action A is a binary variable indicating the presence of the keyword "theorem", and the outcome Y is a binary variable indicating acceptance or rejection. Since real-world counterfactual outcomes are inaccessible, we follow prior methods by generating synthetic outcomes based on the action A and the title buzziness Z (i.e., whether the title contains "deep", "neural", "embed", or "adversarial net"). For example, $z = 1$ and $a = 1$ likely correspond to a deep learning paper that includes a theorem, while $z = 0$ and $a = 1$ may represent a theoretical machine learning paper or a deep learning paper with a theorem but without a buzzy title.

Define the propensity function $\pi(z)$ as the proportion of data samples with $a_i = 1$ among those satisfying $z_i = z$. Let β be a parameter controlling the level of confounding between title buzziness and the outcome. Following Veitch et al. (2020), we generate outcomes using the model:

$$Y_i \sim \text{Bernoulli}(\sigma(0.25a_i + \beta(\pi(z_i) - 0.2))).$$

Since evaluating any causal effect model requires counterfactual outcomes that are inaccessible in real-world data, we use a semi-synthetic setting, where the covariates are real-world data and the labels are generated according to patterns in the data, albeit synthetically. Veitch et al. (2020) have established a correlation between title buzziness and the text.

Following the original experimental design, we report the Average Treatment Effect on the Treated (ATT),

$$ATT \coloneqq p(Y = 1 \mid \mathsf{do}(A = 1),\, A = 1) - p(Y = 1 \mid \mathsf{do}(A = 0),\, A = 1),$$

across three confounding levels: low, medium, and high. A positive ATT indicates that including a theorem increases a paper's chance of acceptance. For larger values of β, the outcome becomes more correlated with title buzziness Z rather than the action A, so the ground truth ATT is smaller.

We compare our proposed approach to a non-autoregressive MLP baseline and Causal-BERT (C-BERT) from Veitch et al. (2020).[7] Like C-BERT, we fine-tune a pre-trained BERT model on our sequencified representations for a fair comparison. Additionally, we evaluate GPT-2 (referred to as GPT), another pre-trained LLM with a comparable parameter size to BERT (Radford et al., 2019).

BERT is trained using masked language modeling (MLM) and next-sentence prediction objectives. MLM randomly masks a fraction of input tokens and trains the model to predict them. GPT is trained with a next-token prediction objective. To adapt BERT for this setting, we randomly sample subsection of the abstract during training and mask the final token to fine-tune it as a next-token prediction model.

---

[7] C-BERT learns causally sufficient embeddings—low-dimensional document representations that preserve sufficient information for causal identification and enable efficient causal effect estimation.

As shown in Table 1, our approach significantly outperforms C-BERT and other benchmarks, including the baseline MLP.[8] The primary distinction between our approach and C-BERT is that we jointly learn representations and outcome predictions within a single model, whereas C-BERT uses additional architectural layers for multiple objective functions.

Our proposed framework leverages the existing knowledge in pre-trained LLMs to accurately estimate causal quantities. While fine-tuning GPT yields successful results, training the model from scratch fails to identify causal effects because the model lacks prior understanding of the text domain. We also demonstrate that our results are robust to the size of the pre-trained LLM in Appendix C. By utilizing pre-trained language models, our approach outperforms non-autoregressive causal methods and proves more effective for a wider range of CI tasks.

7 Conclusion

In this work, we introduce an AR framework for CI that handles high-dimensional confounders and combinatorially large action spaces. Our proposed method, called *sequencification*, transforms data into a linear sequence of tokens based on a known causal diagram. By training a single AR model on sequencified data, we learn conditional distributions between variables in the graph. The framework enables efficient sampling and approximation of several interventional distributions in a unified manner.

We validate the effectiveness of our method in inferring causal effects across three diverse settings: maze navigation, chess endgames, and paper acceptance rates. By accommodating high-dimensional confounders and combinatorially large action sequences, our framework improves the flexibility of CI for a broader range of applications.

Our approach has two main limitations. First, it requires the full causal graph to be known exactly, with all variables observed. A possible solution for handling unobserved values is to impute unconfounded missing data using a mask token. Second, our method supports conditioning or intervening only on variable prefixes. While non-prefix interventions is difficult, prior work has explored strategies to address this challenge (Donahue et al., 2020; Welleck et al., 2019; Berenberg et al., 2022). We leave the investigation of solutions to these limitations for future work.

References

Daniel Berenberg, Jae Hyeon Lee, Simon Kelow, Ji Won Park, Andrew Watkins, Vladimir Gligorijević, Richard Bonneau, Stephen Ra, and Kyunghyun Cho. Multi-segment preserving sampling for deep manifold sampler, 2022.

Lili Chen, Kevin Lu, Aravind Rajeswaran, Kimin Lee, Aditya Grover, Michael Laskin, Pieter Abbeel, Aravind Srinivas, and Igor Mordatch. Decision transformer: Reinforcement learning via sequence modeling, 2021.

Aakanksha Chowdhery, Sharan Narang, Jacob Devlin, Maarten Bosma, Gaurav Mishra, and Adam Roberts et al. Palm: Scaling language modeling with pathways. *Journal of Machine Learning Research*, 24(240): 1–113, 2023. URL `http://jmlr.org/papers/v24/22-1144.html`.

William G. Cochran and Donald B. Rubin. Controlling bias in observational studies: A review. *The Indian Journal of Statistics, Series A*, 35:417–446, 1973. doi: JSTOR,http://www.jstor.org/stable/25049893.

Chris Donahue, Mina Lee, and Percy Liang. Enabling language models to fill in the blanks, 2020.

Alexander D'Amour, Peng Ding, Avi Feller, Lihua Lei, and Jasjeet Sekhon. Overlap in observational studies with high-dimensional covariates. *Journal of Econometrics*, 221(2):644–654, 2021.

Naoki Egami, Christian J Fong, Justin Grimmer, Margaret E Roberts, and Brandon M Stewart. How to make causal inferences using texts. *Science Advances*, 8(42):eabg2652, 2022.

---

[8] We discuss the strong performance despite differences between synthetic and real-world causal graphs in Appendix C.

Sergio Garrido, Stanislav Borysov, Jeppe Rich, and Francisco Pereira. Estimating causal effects with the neural autoregressive density estimator. *Journal of Causal Inference*, 9(1):211–228, 2021. doi: doi:10.1515/jci-2020-0007. URL `https://doi.org/10.1515/jci-2020-0007`.

Lin Gui and Victor Veitch. Causal estimation for text data with (apparent) overlap violations. *arXiv preprint arXiv:2210.00079*, 2022.

Kshitij Gupta, Benjamin Th'erien, Adam Ibrahim, Mats L. Richter, Quentin G. Anthony, Eugene Belilovsky, Irina Rish, and Timothée Lesort. Continual pre-training of large language models: How to (re)warm your model? *ArXiv*, abs/2308.04014, 2023. URL `https://api.semanticscholar.org/CorpusID:260704601`.

Paul W. Holland. Statistics and causal inference. *Journal of the American Statistical Association*, 81(396): 945–960, 1986. doi: 10.1080/01621459.1986.10478354. URL `https://www.tandfonline.com/doi/abs/10.1080/01621459.1986.10478354`.

Daniel jiwoong Im Im, Kyunghyun Cho, and Narges Razavian. Causal effect variational autoencoder with uniform treatment for overcoming covariate shifts. In *arXiv preprint arXiv:2111.08656*, 2021.

Michael Janner, Qiyang Li, and Sergey Levine. Offline reinforcement learning as one big sequence modeling problem. In M. Ranzato, A. Beygelzimer, Y. Dauphin, P.S. Liang, and J. Wortman Vaughan (eds.), *Advances in Neural Information Processing Systems*, volume 34, pp. 1273–1286. Curran Associates, Inc., 2021. URL `https://proceedings.neurips.cc/paper_files/paper/2021/file/099fe6b0b444c23836c4a5d07346082b-Paper.pdf`.

Fredrik D. Johansson, Nathan Kallus, Uri Shalit, and David A. Sontag. Learning weighted representations for generalization across designs. *arXiv: Machine Learning*, 2018.

Dongyeop Kang, Waleed Ammar, Bhavana Dalvi, Madeleine van Zuylen, Sebastian Kohlmeier, Eduard Hovy, and Roy Schwartz. A dataset of peer reviews (PeerRead): Collection, insights and NLP applications. In Marilyn Walker, Heng Ji, and Amanda Stent (eds.), *Proceedings of the 2018 Conference of the North American Chapter of the Association for Computational Linguistics: Human Language Technologies, Volume 1 (Long Papers)*, pp. 1647–1661, New Orleans, Louisiana, June 2018. Association for Computational Linguistics. doi: 10.18653/v1/N18-1149. URL `https://aclanthology.org/N18-1149`.

Katherine A. Keith, David Jensen, and Brendan O'Connor. Text and causal inference: A review of using text to remove confounding from causal estimates, 2020.

Murat Kocaoglu, Karthikeyan Shanmugam, and Elias Bareinboim. Experimental design for learning causal graphs with latent variables. In I. Guyon, U. Von Luxburg, S. Bengio, H. Wallach, R. Fergus, S. Vishwanathan, and R. Garnett (eds.), *Advances in Neural Information Processing Systems*, volume 30. Curran Associates, Inc., 2017. URL `https://proceedings.neurips.cc/paper/2017/file/291d43c696d8c3704cdbe0a72ade5f6c-Paper.pdf`.

Daniel Kumor, Junzhe Zhang, and Elias Bareinboim. Sequential causal imitation learning with unobserved confounders. In M. Ranzato, A. Beygelzimer, Y. Dauphin, P.S. Liang, and J. Wortman Vaughan (eds.), *Advances in Neural Information Processing Systems*, volume 34, pp. 14669–14680. Curran Associates, Inc., 2021. URL `https://proceedings.neurips.cc/paper/2021/file/7b670d553471ad0fd7491c75bad587ff-Paper.pdf`.

Hugo Larochelle and Iain Murray. The neural autoregressive distribution estimator. In Geoffrey Gordon, David Dunson, and Miroslav Dudík (eds.), *Proceedings of the Fourteenth International Conference on Artificial Intelligence and Statistics*, volume 15 of *Proceedings of Machine Learning Research*, pp. 29–37, Fort Lauderdale, FL, USA, 11–13 Apr 2011. PMLR. URL `https://proceedings.mlr.press/v15/larochelle11a.html`.

Tianyu Liu, Yuchen Eleanor Jiang, Nicholas Monath, Ryan Cotterell, and Mrinmaya Sachan. Autoregressive structured prediction with language models. In Yoav Goldberg, Zornitsa Kozareva, and Yue Zhang (eds.), *Findings of the Association for Computational Linguistics: EMNLP 2022*, pp. 993–1005, Abu Dhabi, United Arab Emirates, December 2022. Association for Computational Linguistics. doi: 10.18653/v1/2022.findings-emnlp.70. URL `https://aclanthology.org/2022.findings-emnlp.70`.

Christos Louizos, Uri Shalit, Joris Mooij, David Sontag, Richard Zemel, and Max Welling. Causal effect inference with deep latent-variable models. In *arXiv preprint arXiv:1705.08821*, 2017.

Zhenyu Lu, Yurong Cheng, Mingjun Zhong, George Stoian, Ye Yuan, and Guoren Wang. *Causal Effect Estimation Using Variational Information Bottleneck*, pp. 288–296. 12 2022. ISBN 978-3-031-20308-4. doi: 10.1007/978-3-031-20309-1-25.

Ricardo Pio Monti, Ilyes Khemakhem, and Aapo Hyvarinen. Autoregressive flow-based causal discovery and inference, 2020.

Reagan Mozer, Luke Miratrix, Aaron Russell Kaufman, and L Jason Anastasopoulos. Matching with text data: An experimental evaluation of methods for matching documents and of measuring match quality. *Political Analysis*, 28(4):445–468, 2020.

Judea Pearl. *Causality: Models, Reasoning and Inference*. Cambridge University Press, USA, 2nd edition, 2009. ISBN 052189560X.

Judea Pearl. An introduction to causal inference. *The international journal of biostatistics*, 6:1557–4679, 2010.

Alec Radford, Jeff Wu, Rewon Child, David Luan, Dario Amodei, and Ilya Sutskever. Language models are unsupervised multitask learners. 2019.

Md Musfiqur Rahman and Murat Kocaoglu. Modular learning of deep causal generative models for high-dimensional causal inference. *ArXiv*, abs/2401.01426, 2024. URL `https://proceedings.mlr.press/v235/rahman24a.html`.

Margaret E Roberts, Brandon M Stewart, and Richard A Nielsen. Adjusting for confounding with text matching. *American Journal of Political Science*, 64(4):887–903, 2020.

Uri Shalit, Fredrik D. Johansson, and David Sontag. Estimating individual treatment effect: Generalization bounds and algorithms. ICML'17, pp. 3076–3085. JMLR.org, 2017.

Kun Sheng, Zhongqing Wang, Qingqing Zhao, Xiaotong Jiang, and Guodong Zhou. A unified framework for synaesthesia analysis. In Houda Bouamor, Juan Pino, and Kalika Bali (eds.), *Findings of the Association for Computational Linguistics: EMNLP 2023*, pp. 6038–6048, Singapore, December 2023. Association for Computational Linguistics. doi: 10.18653/v1/2023.findings-emnlp.401. URL `https://aclanthology.org/2023.findings-emnlp.401`.

Dhanya Sridhar and Lise Getoor. Estimating causal effects of tone in online debates. In *Proceedings of the Twenty-Eighth International Joint Conference on Artificial Intelligence*, 2019.

Jin Tian and Judea Pearl. A general identification condition for causal effects. In *AAAI/IAAI*, 2002. URL `https://ftp.cs.ucla.edu/pub/stat_ser/R290-A.pdf`.

Haoqin Tu and Yitong Li. An overview on controllable text generation via variational auto-encoders. *ArXiv*, abs/2211.07954, 2022. URL `https://api.semanticscholar.org/CorpusID:253523104`.

Ashish Vaswani, Noam Shazeer, Niki Parmar, Jakob Uszkoreit, Llion Jones, Aidan N Gomez, Łukasz Kaiser, and Illia Polosukhin. Attention is all you need. *Advances in neural information processing systems*, 30, 2017.

Victor Veitch, Dhanya Sridhar, and David M. Blei. Using text embeddings for causal inference. *ArXiv*, abs/1905.12741, 2019. URL `https://api.semanticscholar.org/CorpusID:170079051`.

Victor Veitch, Dhanya Sridhar, and David Blei. Adapting text embeddings for causal inference. In Jonas Peters and David Sontag (eds.), *Proceedings of the 36th Conference on Uncertainty in Artificial Intelligence (UAI)*, volume 124 of *Proceedings of Machine Learning Research*, pp. 919–928. PMLR, 03–06 Aug 2020. URL `https://proceedings.mlr.press/v124/veitch20a.html`.

Oriol Vinyals, Lukasz Kaiser, Terry Koo, Slav Petrov, Ilya Sutskever, and Geoffrey Hinton. Grammar as a foreign language. In *NIPS*, 2015. URL `http://arxiv.org/abs/1412.7449`.

Yixin Wang and Michael I. Jordan. Desiderata for representation learning: A causal perspective, 2021.

Sean Welleck, Kianté Brantley, Hal Daumé Iii, and Kyunghyun Cho. Non-monotonic sequential text generation. In Kamalika Chaudhuri and Ruslan Salakhutdinov (eds.), *Proceedings of the 36th International Conference on Machine Learning*, volume 97 of *Proceedings of Machine Learning Research*, pp. 6716–6726. PMLR, 09–15 Jun 2019. URL `https://proceedings.mlr.press/v97/welleck19a.html`.

Kevin Muyuan Xia, Yushu Pan, and Elias Bareinboim. Neural causal models for counterfactual identification and estimation. In *International Conference on Learning Representations*, 2023. URL `https://openreview.net/pdf?id=vouQcZS8KfW`.

Mengwei Xu, Wangsong Yin, Dongqi Cai, Rongjie Yi, Daliang Xu, Qipeng Wang, Bingyang Wu, Yihao Zhao, Chen Yang, Shihe Wang, et al. A survey of resource-efficient llm and multimodal foundation models. *arXiv preprint arXiv:2401.08092*, 2024.

Peiyuan Zhang, Guangtao Zeng, Tianduo Wang, and Wei Lu. Tinyllama: An open-source small language model, 2024.

Kailiang Zhong, Fengtong Xiao, Yan Ren, Yaorong Liang, Wenqing Yao, Xiaofeng Yang, and Ling Cen. Descn: Deep entire space cross networks for individual treatment effect estimation. *Proceedings of the 28th ACM SIGKDD Conference on Knowledge Discovery and Data Mining*, 2022.

A Appendix

The maze experiments were conducted on a single NVIDIA Tesla T4. All models for the chess and `PeerRead` experiments were trained on a single NVIDIA GeForce RTX 3090 in four and eight hours respectively.

Maze experiments. The maze dataset comprises 10,000 sequencified data points. We use a vanilla transformer with 3 layers, 8 attention heads, and a hidden dimension of 64. For training, we use the Adam optimizer with a batch size of 64. The CI model is trained for 6,250 iterations, while the offline RL model is trained for 5,000 iterations.

Chess endgame experiments. We use a 512-dimensional vanilla transformer with 6 layers and 8 attention heads. The model is trained on a next-token prediction task using the sequencified representation. Training runs for 200 epochs with the Adam optimizer, a batch size of 4096, and a learning rate chosen to be as large as possible without overfitting.

For the training dataset, we sample 500,000 two-move chess games per dataset based on Black's policy function. The test dataset includes every game from all 223,660 legal starting positions and all four possible Black actions (king-king, king-rook, rook-king, rook-rook). We sequencify the data by assigning a unique token to each square, legal king and rook move, and outcome.

`PeerRead` experiments. We fine-tuned our models using pre-trained BERT and GPT base model checkpoints.[9] For BERT, we employed a two-phase training process similar to C-BERT. In the first phase, we trained BERT to generate abstracts, followed by a second phase where it learned to generate full sequences, including both actions and outcomes. GPT, having been pre-trained on next-token prediction, required only a single training phase. This approach ensures a gradual refinement of the generative capabilities specifically tailored to the `PeerRead` corpus. For all training phases, we trained for 100 epochs using the Adam optimizer with a batch size of 16. The learning rate was set as high as possible without overfitting.

B Chess endgame potential outcome estimates

Table 2 compares the potential outcome values for all actions, presenting both exact model estimates and approximate model estimates. Our AR model performs similarly to the baseline across both metrics. Predictions from the model aligns with the ground truth answer to our counterfactual query: on average, moving the rook twice leads to the fastest checkmate.

Table 2: Chess endgame potential outcome estimates for all actions. The outcome represents the number of additional moves required to checkmate White. Since Black aims to achieve checkmate as quickly as possible, lower values are desired.

		Potential outcome (Error %)			
		king-king	king-rook	rook-king	rook-rook
Ground truth		22.76	20.18	20.48	17.27
MLP exact	RCT	**22.51 (1.1%)**	**19.96 (1.1%)**	19.85 (3.1%)	17.08 (1.1%)
	non-RCT$_1$	22.40 (1.6%)	19.85 (1.6%)	20.01 (2.3%)	17.10 (1.0%)
	non-RCT$_2$	22.24 (2.3%)	19.90 (1.4%)	19.69 (3.9%)	17.14 (0.8%)
MLP approx.	RCT	22.17 (2.6%)	19.45 (3.6%)	17.72 (13%)	16.18 (6.3%)
	non-RCT$_1$	22.04 (3.2%)	19.32 (4.3%)	17.91 (13%)	16.12 (6.6%)
	non-RCT$_2$	21.86 (4.0%)	19.31 (4.3%)	17.86 (13%)	16.18 (6.3%)
AR exact	RCT	22.38 (1.7%)	19.75 (2.1%)	19.96 (2.5%)	16.95 (1.9%)
	non-RCT$_1$	22.48 (1.2%)	19.87 (1.5%)	**20.08 (2.0%)**	17.08 (1.1%)
	non-RCT$_2$	22.05 (3.1%)	19.88 (1.5%)	19.80 (3.3%)	**17.17 (0.6%)**
AR approx.	RCT	21.90 (3.8%)	19.19 (4.9%)	17.62 (14%)	15.97 (7.5%)
	non-RCT$_1$	22.03 (3.2%)	19.33 (4.2%)	17.95 (12%)	16.15 (6.5%)
	non-RCT$_2$	21.79 (4.3%)	19.29 (4.4%)	17.54 (14%)	16.31 (5.6%)

---

[9] BERT-Base is available at `https://huggingface.co/google/bert_uncased_L-12_H-768_A-12`, and GPT is available at `https://huggingface.co/openai-community/gpt2`.

In Figure 6, we present the potential outcome graphs for the remaining three actions: king-king, king-rook, and rook-rook. The model behavior on these actions closely aligns with the observations for rook-king in Figure 5. Across multiple interventions, Monte Carlo sampling improves potential outcome estimates when only a subset of the test data is available. Thus, our approach not only effectively models outcomes but also leverages Monte Carlo sampling to enhance predictions in limited data scenarios.

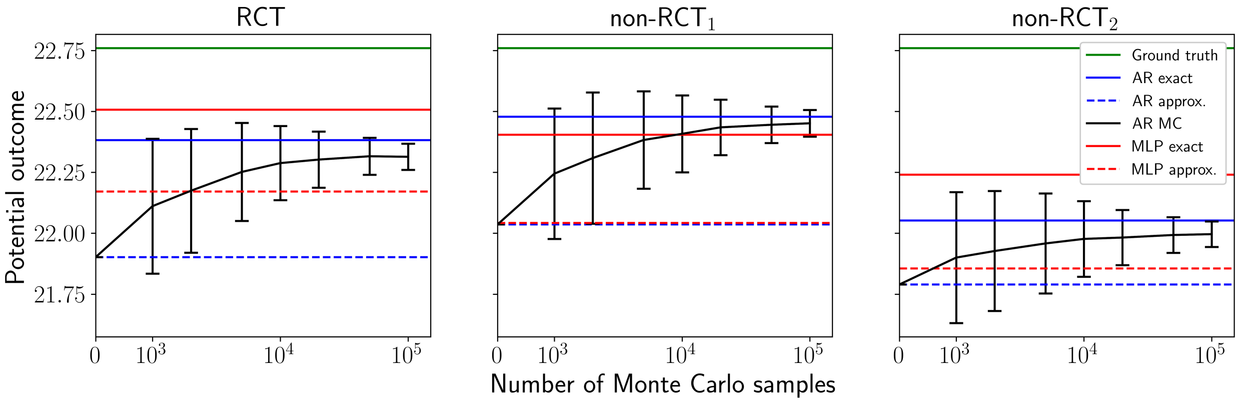

(a) King-king potential outcome estimates.

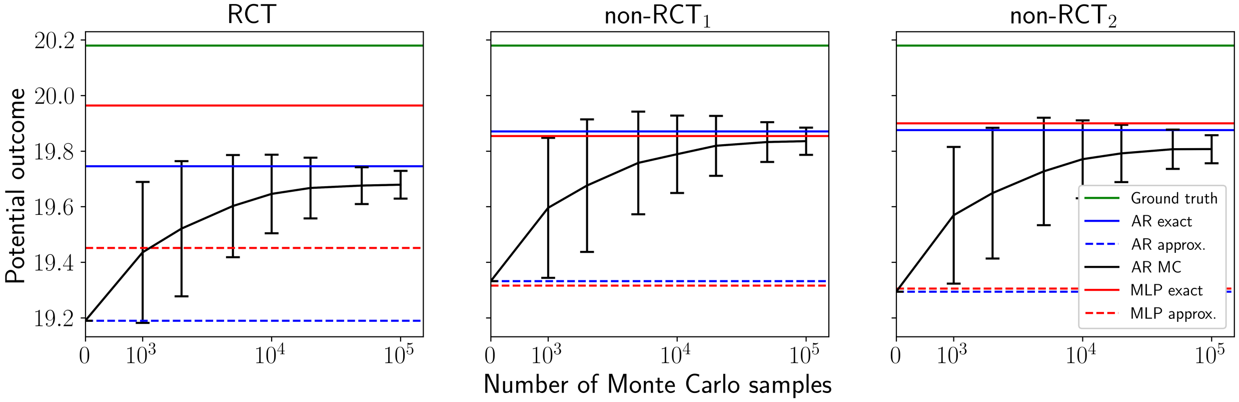

(b) King-rook potential outcome estimates.

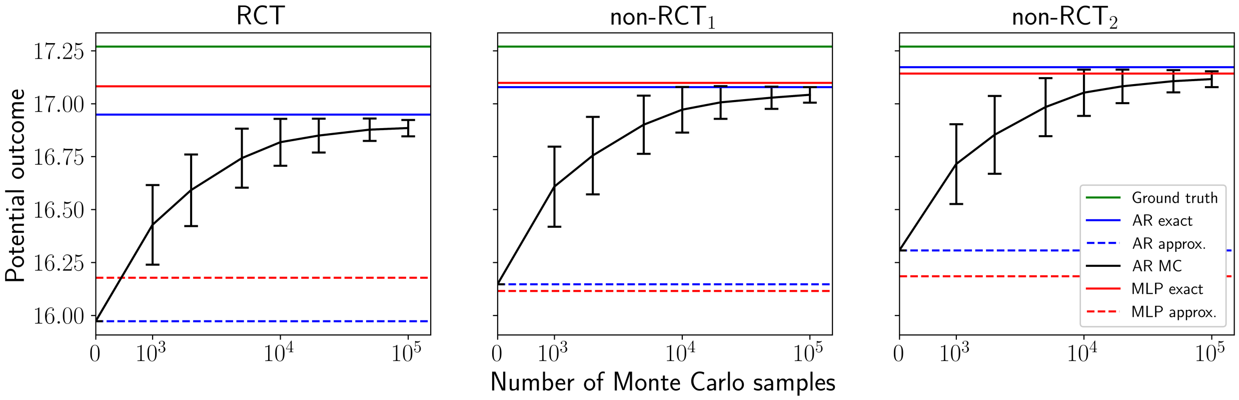

(c) Rook-rook potential outcome estimates.

Figure 6: Potential outcome estimates for (a) king-king, (b) king-rook, and (c) rook-rook actions. Similar to the rook-king intervention, sampling from $p_\theta(X)$ enables the AR Monte Carlo estimate to approach the AR exact estimate.

Table 3: Accuracy and balanced accuracy of title buzziness prediction from the abstract using logistic regression.

	Acc.	Balanced acc.
BoW	87.95%	73.27%
BERT	88.57%	77.91%
GPT2	89.18%	81.00%

Table 4: `PeerRead` ATT estimates for GPT small, medium, and large, with relative error shown in parentheses.

		Confounding level		
	# params	Low	Medium	High
Ground truth		0.062	0.059	0.028
GPT-small	117M	0.050 (20%)	0.044 (25%)	0.020 (29%)
GPT-medium	345M	**0.052 (16%)**	0.053 (10%)	0.038 (36%)
GPT-large	774M	0.051 (18%)	**0.054 (8%)**	**0.021 (25%)**

C `PeerRead` extra experiments

To illustrate the positive predicted ATT on the `PeerRead` dataset, we compare $p_\theta(Y = 1 \mid A = 1, X)$ and $p_\theta(Y = 1 \mid A = 0, X)$ predicted by GPT in Figure 7. Our model consistently favors papers containing theorems regardless of title buzziness.

Furthermore, we examine why our model performs well when the outcome is generated from Z and A while the input is derived from X and A. To quantify the correlation between title buzziness and the abstract, we train a logistic regression model to predict Z from X. For each model, we extract the final hidden layer output as a dense vectorized representation of the abstract. As a baseline, we train a separate logistic regression model using the bag-of-words (BoW) representation of X. Table 3 shows a strong correlation between X and Z, explaining the high accuracy of our potential outcome estimations.

We also examine the impact of pre-trained language model size on effect estimation accuracy using three versions of GPT . Table 4 indicates that larger models generally yield more accurate estimates.

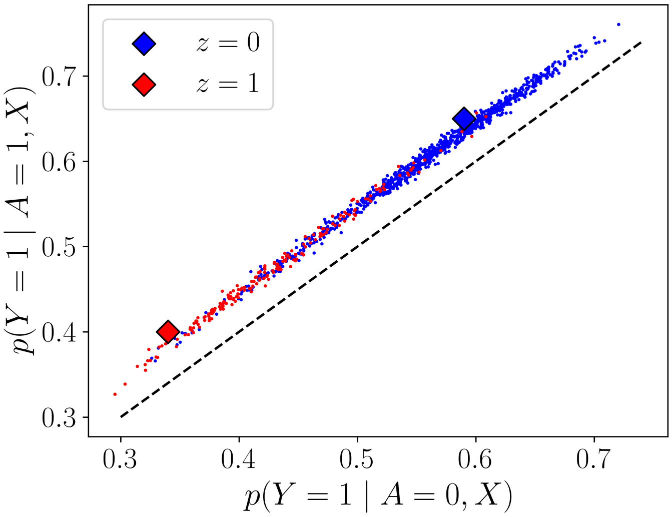

Figure 7: Conditional outcome distributions given $A = 0$ vs. $A = 1$ for medium confounding data.